Highly efficient continuous-wave laser operation of laser diode-pumped Nd,Y:CaF_2 crystals

Qian Zhang (张 倩)[1,4], Liangbi Su (苏良碧)[1,*], Dapeng Jiang (姜大朋)[1], Fengkai Ma (马凤凯)[1,4], Zhipeng Qin (覃志鹏)[2], Guoqiang Xie (谢国强)[2], Jiangang Zheng (郑建刚)[3], Qinghua Deng (邓青华)[3], Wanguo Zheng (郑万国)[3], Liejia Qian (钱列加)[2], and Jun Xu (徐 军)[1,]**

[1]*Key Laboratory of Transparent and Opto-functional Inorganic Materials, Shanghai Institute of Ceramics, Chinese Academy of Sciences, Shanghai 201800, China*

[2]*Key Laboratory for Laser Plasmas (Ministry of Education), Department of Physics and Astronomy, Shanghai Jiao Tong University, Shanghai 200240, China*

[3]*Research Center of Laser Fusion, China Academy of Engineering Physics, Mianyang 621900, China*

[4]*University of Chinese Academy of Sciences, Beijing 100049, China*

**Corresponding author: su_lb@163.com; **corresponding author: xujun@mail.shcnc.ac.cn*

Received January 4, 2015; accepted April 29, 2015; posted online June 4, 2015

The effect of co-doping Y^{3+} and the doping concentration of Nd^{3+} on the spectroscopic properties and laser performance of Nd:CaF_2 crystals are investigated systematically. For a 0.5% Nd:CaF_2 crystal, the emission lifetime at 1.06 μm increases from 18 to 361 μs by co-doping 10 at.% Y^{3+}, while the emission cross section increases to 4.27×10^{-20} cm^2 at 1054 nm. With a 10 at.% doping concentration of Y^{3+}, Nd, Y:CaF_2 crystals concentrate emission bands that peak at 1054 nm with shoulders at 1063 nm, and FWHM at about 30 nm. A diode-pumped, highly efficient laser operation is obtained with 0.5% Nd, 10% Y:CaF_2 and 0.6% Nd, 10% Y:CaF_2 crystals, with slope efficiencies over 30% and 27%, respectively, and a maximum output power up to 901 mW.

OCIS codes: 140.0140, 160.0160, 300.0300.

doi: 10.3788/COL201513.071402.

The demonstration of a laser operation in calcium fluoride doped with samarium[1] and uranium ions[2] has stimulated great interest in alkaline earth fluorides activated with lanthanide ions, especially trivalent neodymium ions. Unfortunately, early works on this subject revealed that the luminescence of neodymium ion clusters, which are easily formed in these crystals, has been completely quenched by the incoherent dipole–dipole energy transfer process[3]. As a consequence, rare earth-doped alkaline earth fluorides were discarded as laser materials.

Recently, however, interest in these systems has been renewed. The incorporation of Y^{3+}, La^{3+}, and Sc^{3+} ions resulted in the dissociation of the Nd^{3+}–Nd^{3+} quenching pairs in clusters, thereby critically reducing the luminescence quenching in neodymium-doped alkaline earth fluorides[4–8]. Nd, Y:SrF_2 crystals have achieved some interesting laser performances[9–11]. Continuous-wave (CW) laser operation in a Nd^{3+} (2 at.%) doped Y^{3+}:CaF_2 crystal pumped by a CW Ti:sapphire laser has been observed, although the output power and efficiency were relatively low[12]. Laser slope efficiencies of 50% in a 0.5% Nd^{3+}, 5% Lu^{3+}:CaF_2 crystal and of 33% in a 1% Nd^{3+}, 5% Y^{3+}:CaF_2 crystal have been achieved when pumping with a CW Ti:sapphire laser. The former sample, which had a 400 μm fiber-coupled laser-diode pumped laser, showed a slope efficiency of 20%[13].

In this work, the effects of Y^{3+} co-doping and the doping concentrations of Nd^{3+} on the spectra properties and laser performance of Nd, Y:CaF_2 crystals were investigated. This research will offer valuable data to find the optimal proportions of Nd^{3+}/Y^{3+} to achieve good laser performance. With doping concentrations of 0.5% Nd^{3+} and 10% Y^{3+}, a highly efficient CW laser operation is obtained in a Nd, Y:CaF_2 crystal with a slope efficiency over 30% and an output power of 0.9 W. The slope efficiency of 27.82% was also obtained in a 0.6% Nd, 10% Y:CaF_2 crystal.

The 0.5% Nd:CaF_2 and $x(x = 0.4\%, 0.5\%, 0.6\%, 0.8\%)$ Nd, 10% Y:CaF_2 single crystals were grown using the temperature gradient technique method as described in Ref. [14]. The raw materials are NdF_3 (99.99%), CaF_2 (99.99%), YF_3 (99.99%), and PbF_2 (99%). Nd^{3+} and Y^{3+} co-doped CaF_2 samples were obtained by cutting and double-face polishing with a thickness of 2 mm. The real concentrations of Nd^{3+} and Y^{3+} were measured by an inductively coupled plasma atomic emission spectrometry analysis with a measurement error of less than 5%. The segregation coefficients of the Nd^{3+} and Y^{3+} ions are about 1.11 and 0.97, respectively. The absorption spectra were recorded by a Jasco V-570 UV/VIS/NIR spectrophotometer. The fluorescence spectra were obtained with a FLSP920 time-resolved fluorimeter grating blazed at 1200 nm and detected by a Hamamatsu near infrared (NIR) photomultiplier tube. The fluorescence decay curves of the samples were obtained by a Tektronix TDS 3052 oscilloscope, and the fluorescence lifetimes were obtained by a fluorescence decay curves fitting.

The room-temperature absorption spectra of the 0.5% Nd:CaF_2 and the 0.5% Nd, 10% Y:CaF_2 crystals are

shown in Fig. 1. The absorption bands corresponding to the different energy levels for the Nd^{3+} ion are shown in Fig. 1(a). The absorption band around 791 nm, which is usually used for diode pumping corresponding to the absorption transition $^4I_{9/2} \rightarrow {}^4F_{5/2} + {}^2H_{9/2}$, is shown in Fig. 1(b). For the 0.5% Nd:CaF_2 crystal, one main peak at 791 nm and two shoulder peaks at 795 and 799 nm are observed. When the 10% YF_3 was co-doped, the strongest absorption band was moved to 797 nm.

The room-temperature emission spectra of the 0.5% Nd:CaF_2 and 0.5% Nd, 10% Y:CaF_2 crystals are shown in Fig. 2. The inset shows an emission band around 1.06 μm, which corresponds to the emission transition $^4F_{3/2} \rightarrow {}^4I_{3/2}$ for the 0.5% Nd:CaF_2 crystal. There are six emission peaks at 1036, 1046, 1062, 1081, 1092, and 1127 nm in the emission spectrum of the single neodymium-doped CaF_2 crystal, indicating the diversity of the Nd^{3+} centers. When the 10% Y^{3+} ion is co-doped, the emission intensity is sharply enhanced. Furthermore, only one relatively broad emission band with a FWHM of

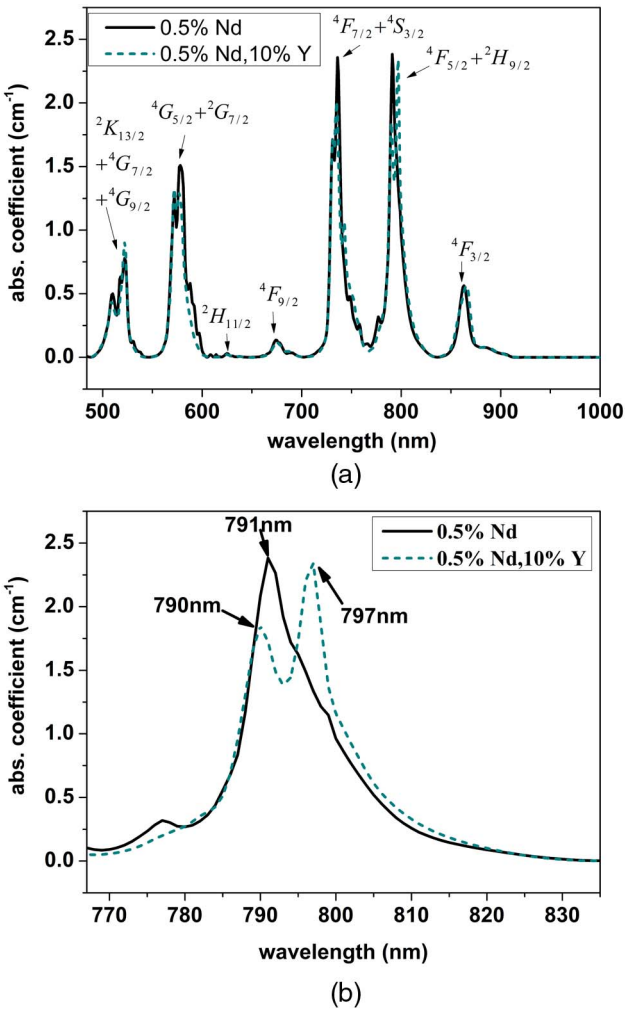

Fig. 1. Room-temperature absorption spectra of (a) the 0.5% Nd:CaF_2 crystal, which is 484–1000 nm and (b) the 0.5% Nd, 10% Y:CaF_2 crystal, which is 767-835 nm.

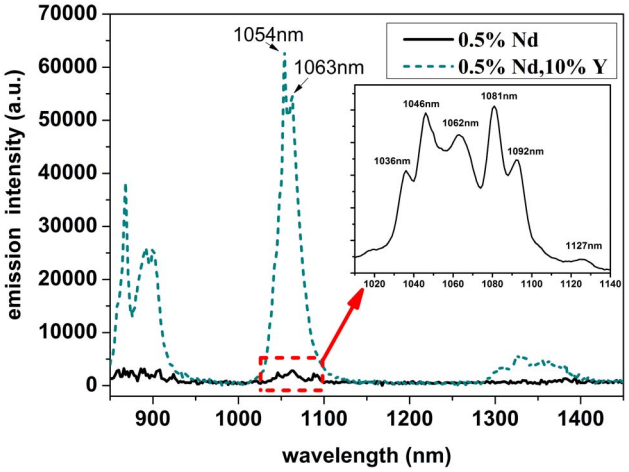

Fig. 2. Room temperature emission spectra of the 0.5% Nd:CaF_2 and 0.5% Nd, 10% Y:CaF_2 crystals.

30 nm can be observed in the Nd, Y:CaF_2 crystal, peaking at 1054 nm with a shoulder at 1063 nm.

The fluorescence lifetimes were measured to be 18.0 ± 0.2 and 361.0 ± 3.2 μs for the 0.5% Nd:CaF_2 and the 0.5% Nd, 10% Y:CaF_2 crystals, respectively. With the addition of the Y^{3+} buffer ions, the quenching effect is greatly suppressed. The $^4F_{3/2}$ radiative emission lifetimes (τ_{rad}) of the Nd^{3+} ion in the crystals were calculated by the Judd–Ofelt formalism[15,16]. The Judd–Ofelt parameters Ω_2, Ω_4, and Ω_6 are obtained from the measured absorption spectra above, as shown in Table 1. Using the Judd–Ofelt parameters, the radiative emission lifetimes were obtained. Then, the emission cross section (σ_{em}) can be calculated using the well-known Fuchtbauer–Ladenburg expression:

$$\sigma_{em}(\lambda) = \frac{\lambda^4}{8\pi c n^2 \Delta\lambda \tau_{rad}}, \quad (1)$$

where τ_{rad} and n stand for the radiative emission lifetime and the refractive index of the material, respectively. The emission cross section of the 0.5% Nd, 10% Y:CaF_2 crystal was calculated to be 4.27×10^{-20} cm^2. The parameters are shown in Table 1.

The absorption spectra of the four samples of Nd, 10% Y:CaF_2 are presented in Fig. 3. The absorption intensity increases with the Nd^{3+} concentrations. However, the absorption cross section first increases and then decreases with a concentration of Nd^{3+} over 0.6%, as shown in Fig. 3(b). The Judd–Ofelt parameters Ω_2, Ω_4, and Ω_6 of these crystals were also obtained, and are listed in Table 2.

Figure 4 shows the emission spectra of the Nd, Y:CaF_2 crystals around 1054 nm, with nearly the same spectrum characteristics and FWHM of about 30 nm.

The fluorescence lifetimes (τ_{exp}) were measured to be 350.0 ± 3.2, 361.0 ± 3.2, 359.0 ± 2.7, and 321.0 ± 3.1 μs for the four Nd, Y:CaF_2 crystals with Nd doping concentrations of 0.4%, 0.5%, 0.6%, and 0.8%, respectively.

Table 1. Judd–Ofelt Parameters $\Omega_2, \Omega_4, \Omega_6$, Maximum Emission Peak (λ_{em}), FWHM ($\Delta\lambda$), Radiative Emission Lifetime (τ_{rad}), Fluorescence Lifetime (τ_{exp}), Fluorescence Quantum Efficiency (η) and Maximum Emission Cross Section (σ_{em}) for 0.5% Nd:CaF_2 and 0.5% Nd, 10% Y:CaF_2 Crystals

Crystal	Ω_2 (10^{-20} cm^2)	Ω_4 (10^{-20} cm^2)	Ω_6 (10^{-20} cm^2)	λ_{em} (nm)	$\Delta\lambda$ (nm)	τ_{rad} (μs)	τ_{exp} (μs)	η (%)	σ_{em} (10^{-20} cm^2)
0.5%Nd:CaF_2	1.1082	3.6337	4.3470	1062	33.21	1091	17.99	1.65	2.28
0.5%Nd, 10%Y:CaF_2	0.1585	3.2329	3.5231	1054	28.03	657.47	361.27	54.95	4.27

Table 2. Spectroscopic Properties of $x(x = 0.4\%, 0.5\%, 0.6\%, 0.8\%)$ Nd, 10% Y:CaF_2 Crystals

Crystal	Ω_2 (10^{-20} cm^2)	Ω_4 (10^{-20} cm^2)	Ω_6 (10^{-20} cm^2)	λ_{em} (nm)	$\Delta\lambda$ (nm)	τ_{rad} (μs)	τ_{exp} (μs)	η (%)	σ_{em} (10^{-20} cm^2)
0.4%Nd, 10%Y:CaF_2	0.6077	2.8032	3.0639	1054	29.99	795.09	350.62	46.19	3.36
0.5%Nd, 10%Y:CaF_2	0.1585	3.2329	3.5231	1054	28.51	657.47	361.27	54.95	4.27
0.6%Nd, 10%Y:CaF_2	0.4121	2.2806	4.0231	1054	28.96	693.22	359.40	51.85	3.99
0.8%Nd, 10%Y:CaF_2	0.3477	2.9516	3.5851	1054	29.98	677.26	320.97	47.39	3.94

The radiative emission lifetimes (τ_{rad}) and emission cross section (σ_{em}) are also calculated and are shown in Table 2. The emission intensity increases when the concentration of Nd^{3+} increases from 0.4% to 0.6%, and then decreases because of the quenching effect. The experimental results agree well with the trends of fluorescence lifetimes. The Nd, 10% Y:CaF_2 crystals with concentrations of Nd of 0.5% and 0.6% have relatively larger absorption and emission cross sections and longer fluorescence lifetimes, which are favorable for higher-efficiency laser operations.

The laser experiment was conducted with the setup shown in Fig. 5. A commercial laser diode (nLight Laser, NL-CN-10.0-793-3-F) was employed as the pump source, and its emission wavelength varied from 791 to 799 nm as the output power increased. The bandwidth of the pump source was 1.5 nm (FWHM). After being collimated and focused by the lens, the pump light was imaged into the crystal with a spot size of 50 μm * 270 μm. Based on the ABCD propagation matrix method, the waist diameter of the laser mode in the crystal was calculated to be 58 μm. Laser experiments were performed with the 0.5% Nd:CaF_2 and the other four Nd, 10% Y:CaF_2 samples. The output mirror transmission is 2%, and concave mirrors M1 and M2 have the same radium of curvature of 10 cm. The laser output powers of the Nd, 10% Y:CaF_2 crystals are depicted in Fig. 6, with a dependence on the absorbed pump power. It should be noted that we could not obtain a laser output in the 0.5% Nd:CaF_2 sample. At the available maximum pump power of 5.09 W, the 0.5% Nd, 10%

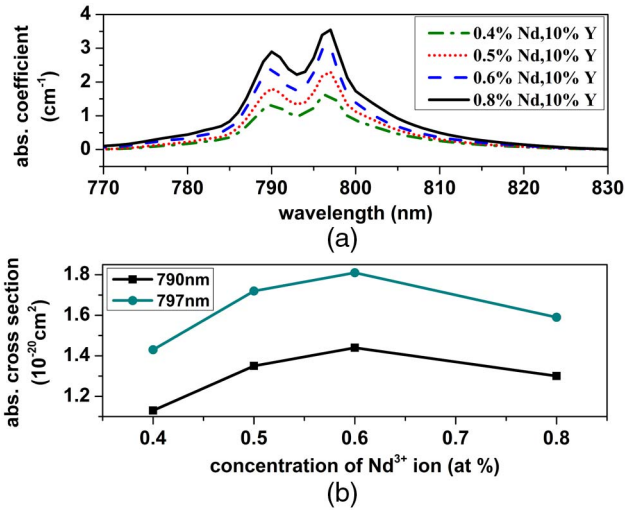

Fig. 3. (a) The room-temperature absorption spectra of the $Nd^{3+4}I_{9/2} \rightarrow {}^4F_{5/2} + {}^2H_{9/2}$ transition. (b) The absorption cross section at 790 and 797 nm for x ($x = 0.4\%$, 0.5%, 0.6%, 0.8%) Nd, 10% Y:CaF_2 crystals.

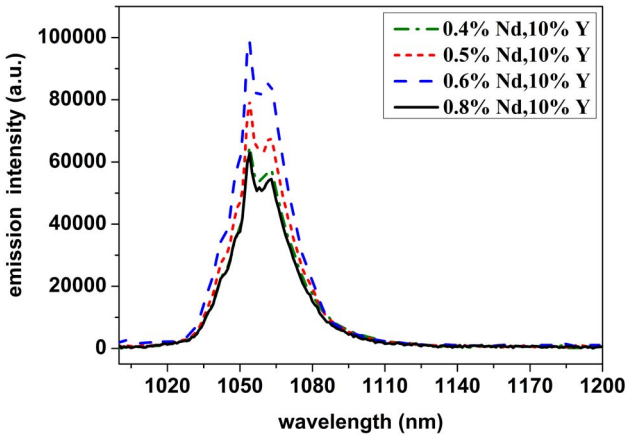

Fig. 4. Room-temperature emission spectra of $x(x = 0.4\%, 0.5\%, 0.6\%, 0.8\%)$ Nd, 10% Y:CaF_2 crystals.

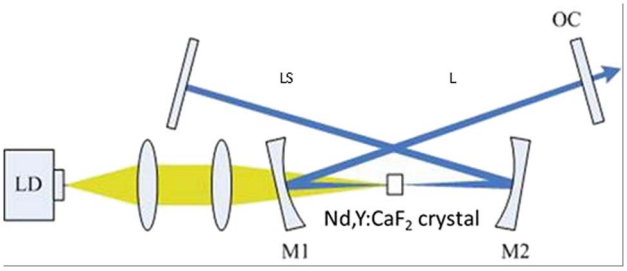

Fig. 5. Schematic of the CW laser setup: LD, laser diode; LS = L = 500 mm; OC: output coupler with a transmission of 2%.

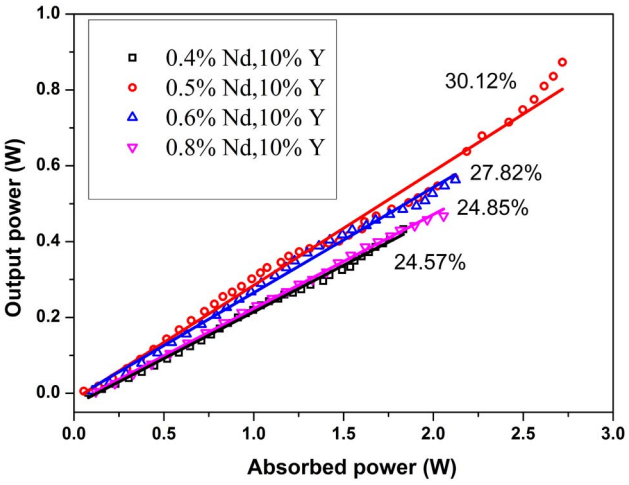

Fig. 6. Laser output power versus absorbed pump power curves for $x(x = 0.4\%, 0.5\%, 0.6\%, 0.8\%)$ Nd, 10% Y:CaF_2 crystals.

Y:CaF_2 crystal absorbed 55% of the pump power. The laser slope efficiencies and maximum output power of the four Nd, 10% Y:CaF_2 crystals are 24.57% and 433 mW, 30.12% and 901 mW, 27.82% and 563 mW, and 24.85% and 468 mW for Nd concentrations of 0.4%, 0.5%, 0.6%, and 0.8%, respectively. Comparing these results with those obtained in similar conditions with a 2% Nd, 2% Y:CaF_2 crystal[12], the laser slope efficiency and maximum output power, which are obtained with the 2.65% transmittive output coupler, increased by 10 times and 57 times, respectively. When compared to a 1% Nd, 5% Y:CaF_2 crystal[13], the laser slope efficiency and maximum output power increased by 1.2 times and 11 times, respectively. The 0.5% Nd, 10% Y:CaF_2 crystal has the largest slope efficiency and maximum output power of 901 mW. A slope efficiency of 27.82% was also obtained in the 0.6% Nd, 10% Y:CaF_2 crystal.

In conclusion, Nd:CaF_2 crystals co-doped with 10% Y^{3+} have favorable spectroscopic properties, with an emission cross section up to 4.27×10^{-20} cm^2, an emission lifetime of 360 μs, and a FWHM of the emission band of 30 nm, respectively. Co-doping Y^{3+} effectively breaks the Nd^{3+} quenching clusters, and optical centers in the samples are changed. A diode-pumped, highly efficient laser operation is obtained with 0.5% Nd, 10% Y:CaF_2 and 0.6% Nd, 10% Y:CaF_2 crystals, with slope efficiencies over 30% and 27.82%, respectively, and a maximum output power up to 901 mW. These will provide valuable information to find the optimal proportions of Nd^{3+}/Y^{3+} to achieve good laser performances. Further experiments with optimized doping concentrations of Nd^{3+} and Y^{3+} ions and an optimized laser cavity are under way.

This work was supported by the National Natural Science Foundation of China under Grant Nos. 61178056, 61422511, and 51432007.

References

1. W. Kaiser, C. G. B. Garrett, and D. L. Wood, Phys. Rev. **123**, 766 (1961).
2. P. P. Sorokin and M. J. Stevenson, Phys. Rev. Lett. **5**, 557 (1960).
3. S. A. Payne, J. A. Caird, L. L. Chase, L. K. Smith, N. D. Nielsen, and W. F. Krupke, J. Opt. Soc. Am. B **8**, 726 (1991).
4. T. P. J. Han, G. D. Jones, and R. W. G. Syme, Phys. Rev. **47**, 14706 (1993).
5. N. E. Kask and L. S. Kornienko, Sov. Phys. JETP. **26**, 331 (1968).
6. A. A. Kaminskii, V. V. Osiko, A. M. Prochoro, and Yu. K. Voronko, Phys. Lett. **22**, 419 (1966).
7. K. S. Bagdasarov, Y. K. Voronko, A. A. Kaminskii, L. V. Krotova, and V. V. Osiko, Phys. Stat. Sol. **12**, 905 (1965).
8. T. T. Basiev, Y. K. Voronko, A. Y. Karasik, V. V. Osiko, and I. A. Shcherbakov, Zh. Eksp. Teor. Fiz. **75**, 66 (1978).
9. J. Guo, J. Li, P. Gao, L. Su, J. Xu, and X. Liang, Chin. Opt. Lett. **12**, 121403 (2014).
10. S. Sun, L. Su, Y. Yuan, and Z. Sun, Chin. Opt. Lett. **11**, 112301 (2013).
11. O. K. Alimov, T. T. Basiev, M. E. Doroshenko, P. P. Fedorov, V. A. Konyushkin, A. N. Nakladov, and V. V. Osiko, Opt. Mater. **34**, 799 (2012).
12. L. B. Su, Q. G. Wang, H. J. Li, G. Brasse, P. Camy, J. L. Doualan, A. Braud, R. Moncorge, Y. Y. Zhan, L. H. Zheng, X. B. Qian, and J. Xu, Laser Phys. Lett. **10**, 035804 (2013).
13. J. L. Doualan, L. B. Su, G. Brasse, A. Benayad, V. Ménard, Y. Y. Zhan, A. Braud, P. Camy, J. Xu, and R. Moncorgé, J. Opt. Soc. Am. B **30**, 3018 (2013).
14. Liangbi Su, Jun Xu, Yongjun Dong, Weiqiao Yang, Guoqing Zhou, and Guangjun Zhao, J. Crystal Growth **261**, 496 (2004).
15. X. Li, X. Liu, L. Zhang, L. Hu, and J. Zhang, Chin. Opt. Lett. **11**, 121601 (2013).
16. Y. Tian, R. R. Xu, L. Y. Zhang, L. L. Hu, and J. J. Zhang, J. Appl. Phys. **108**, 083504 (2010).